Supporting Information for "Three-Dimensional Permeability Inversion Using Convolutional Neural Networks and Positron Emission Tomography"

Zitong Huang[1], Takeshi Kurotori[2,3], Ronny Pini[3], Sally M. Benson[2],

Christopher Zahasky[1]

[1]Department of Geoscience, University of Wisconsin-Madison, Madison, WI, USA

[2]Department of Energy Resources Engineering, Stanford University, Stanford, CA, USA

[3]Department of Chemical Engineering, Imperial College London, London, UK

Contents of this file

1. Table S1 summarizing rock cores used for gathering experimental PET imaging datasets.

2. Figure S1 with illustration of arrival time calculation.

3. Figure S2 with illustration of synthetic porosity-permeability training data relationship.

4. Figure S4 and description of Residual-in-Residual Dense Block.

———

November 3, 2021, 6:50pm

Residual-in-Residual Dense Block

To increase the depth of the networks without the gradient-vanishing or gradient-exploding problem, a residual learning framework was adopted to connect the Dense Blocks in the networks. Instead of directly learning the unreferenced original mapping, the residual connection adopts a skip-connection between blocks that learn residual functions with reference to the layer inputs (He et al., 2016). Suppose x is the input for the current layer and let x denotes the residual. Let $F(x)$ denote the optimal mapping of the current layer and let $R(x)$ denotes the original mapping (or the residual function) of the current layer, and let $F(x)$ $R(x)$ + x. The $F(x)$ is then passed to the next layer, so if the original $R(x)$ of the current layer enlarges the error, the next layer could always refer back to the residual x, which could be considered as skipping the layer that enlarges the error. To the other extreme, if the original mapping $R(x)$ is optimal, the residual x will be set to zero. Therefore, the deeper layer would produce no higher error than the upper layer (He et al., 2016). Compare to the original mapping, it is easier to optimize the residual mapping. The residual-in-residual dense block (RRDB) are composed of a stack of residual dense blocks connected in another residual structure (Wang et al., 2018; Mo et al., 2019). Therefore, the residual learning was used in two levels, resulting in a residual-in-residual structure. For both of the two levels, the desired output is actually denoted as $F(x)\beta \times R(x) + x$, where $\beta \in (0, 1]$ is the residual scaling factor (Wang et al., 2018).

References

He, K., Zhang, X., Ren, S., & Sun, J. (2016). Deep residual learning for image recognition. In *Proceedings of the ieee conference on computer vision and pattern recognition* (Vol. 7, pp. 770–778).

Mo, S., Zabaras, N., Shi, X., & Wu, J. (2019). Integration of Adversarial Au-

toencoders With Residual Dense Convolutional Networks for Estimation of Non-Gaussian Hydraulic Conductivities. *Water Resources Research*, *56*(2), 1–24. doi: 10.1029/2019WR026082

Wang, X., Yu, K., Wu, S., Gu, J., Liu, Y., Dong, C., . . . Tang, X. (2018, 09). Esrgan: Enhanced super-resolution generative adversarial networks. In *European conference on computer vision (eccv)*.

| Sample Name	Core length [cm]	Average Permeability [mD]	Average Porosity [-]
Berea Sandstone	10.0	23	0.20
Indiana limestone	10.3	98	0.17
Edwards Brown limestone	10.3	132	0.41
Ketton limestone	10.0	1920	0.23

Table S1. Table summarizing rock cores used for gathering experimental PET imaging datasets.
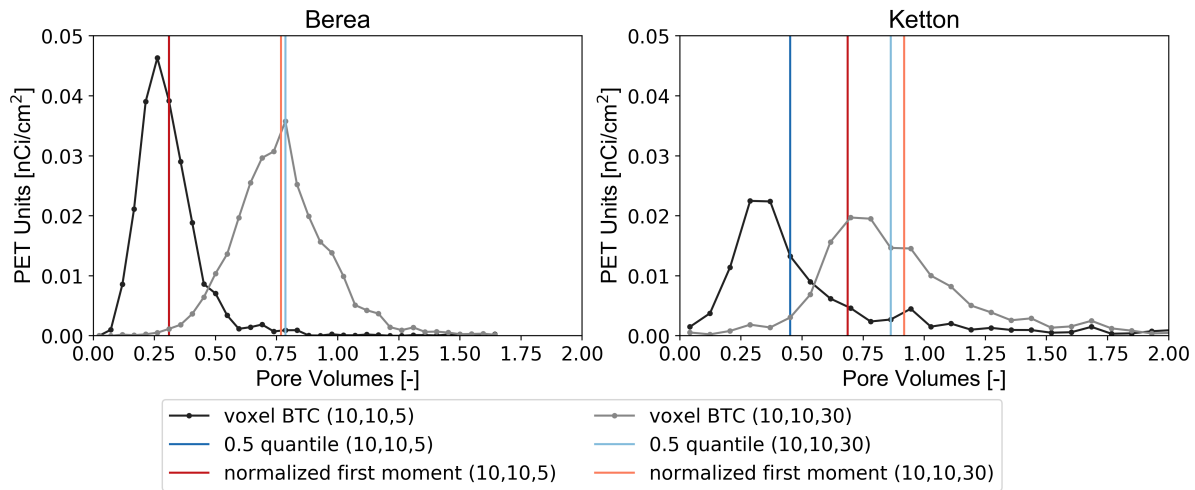
Figure S1. Example breakthrough curves derived from different voxels of the PET scans of the Berea sandstone (left plot) and the Ketton limestone (right plot) experiments. The black lines and darker blue and red lines are for the voxel near the central axis of the core and 1.19 cm from the inlet (voxel coordinate: 10,10,5). The lighter colors correspond to the voxel near the central axis of the core and 7.16 cm from the inlet (voxel coordinate: 10,10,30). While normalized first moments and 0.5 quantiles are very similar in a Berea sandstone, the significant microporosity and resulting solute tailing in the Ketton limestone generates significant delay of the normalized first moment location relative to the 0.5 quantile.

:
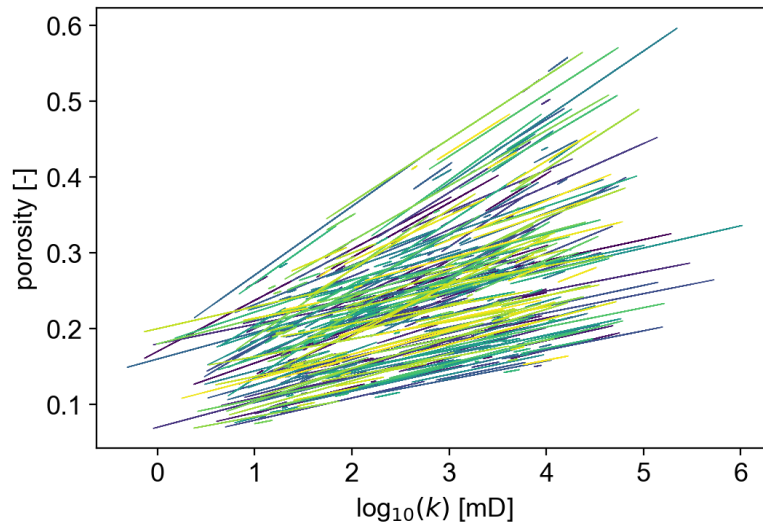
Figure S2. Porosity-permeability relationships for every grid cell of each test set realization using Equation 5 with randomly sampled a and b parameters. Each test set has a different line color and all 500 test datasets are plotted.
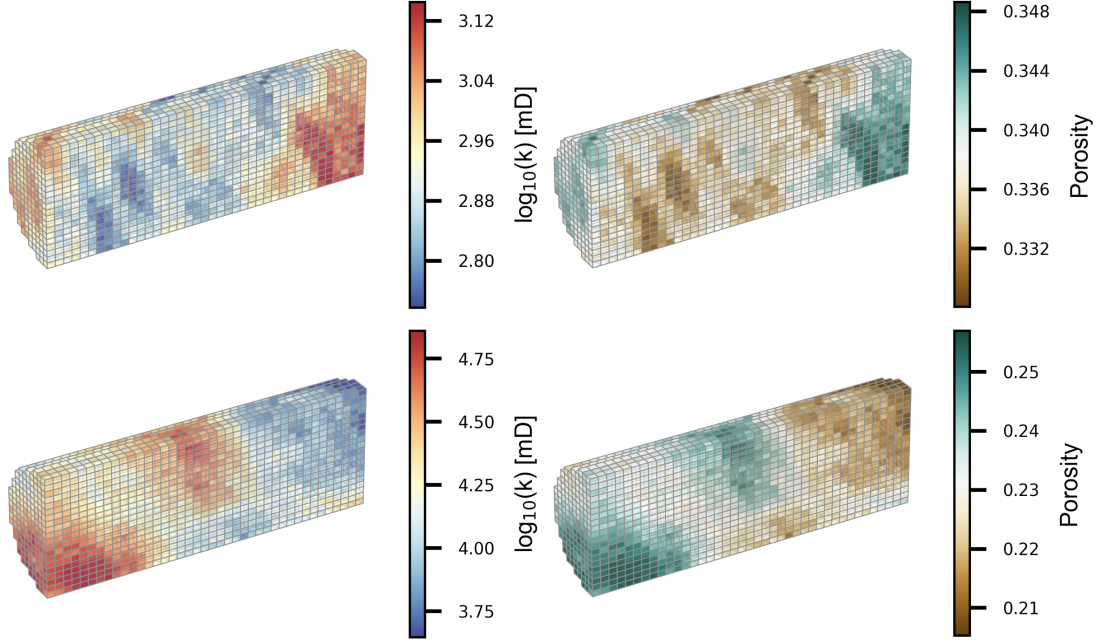
Figure S3. Two test sets of synthetic permeability and corresponding porosity maps used in the second neural network that incorporates heterogeneous porosity. The top row illustrates sample 430 from the test set; the corresponding porosity is generated with $a = 0.4565$ and $b = 19$ using Equation 5. The bottom row illustrates sample 404 from the test set; the corresponding porosity is generated with $a = 0.5407$ and $b = 5$. The grid cells for all models are 0.233 cm $\times$0.233 cm $\times$0.25 cm.
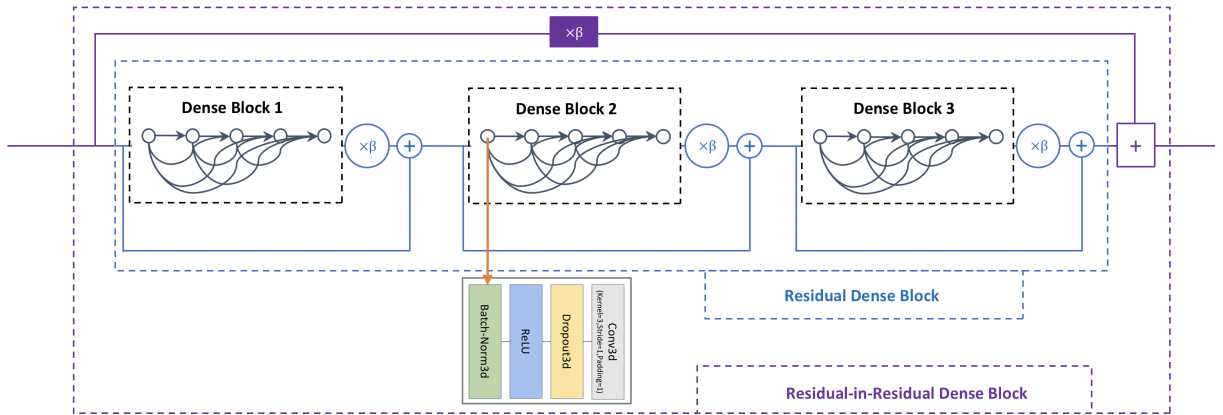
Figure S4. Architecture of the residual-in-residual dense block (Wang et al., 2018; Mo et al., 2019)